An Investigation into Vibration in Switched Reluctance Motors

Pragasen Pillay, *Senior Member, IEEE*, and William (Wei) Cai

***Abstract*—Two disadvantages of the switched reluctance motor (SRM) are its torque ripple and acoustic noise. Previous work on vibration modes and resonant frequencies of the laminations of an 8-6 SRM is extended here to include the effects of the frame. Both a smooth frame and a ribbed frame are examined, and the presence of numerous additional vibratory modes in the ribbed frame demonstrated. Accelerometer tests behind a pole verify some of the theoretical predictions.**

***Index Terms*— Mode shape, resonant frequency, switched reluctance motor, vibration.**

I. Introduction

SWITCHED reluctance motor (SRM) drives are making their presence felt in a variety of applications, from power steering to washing machines to traction. This inroad into the marketplace is based on their advantages over the induction motor in manufacturing, reliability, and robustness.

Two disadvantages of the machine are its torque ripple and acoustic noise. Some previous work has been done in this area, but the research is far from exhausted. The origin of the acoustic noise in SRM's can be broadly classified into two types, mechanical and magnetic. Some of the sources interact with each other and increase the vibration and noise emission. The inverter and the control strategies can affect both mechanical and magnetic noise. The acoustic noise sources are listed as follows.

1) Bearing vibration, due to its construction and any installation errors, causes acoustic noise, which is of purely mechanical origin.
2) SRM's have a doubly salient structure. The rotor poles behave like blades, which cause acoustic noise due to windage.
3) Nonuniform characteristics of materials produce mechanically dynamic unbalance of the rotor and a nonuniform distribution of magnetic flux, which cause both magnetic and mechanical forces on the rotor and result in acoustic noise.
4) Manufacturing asymmetries of the rotor and stator, in particular, a nonuniform air gap, excite asymmetric forces on the rotor.
5) Stator windings that are not installed well or manufactured well can move actively or passively when the motor is running.
6) The currents through the stator windings interact with local magnetic fields to produce forces on the windings, which can excite winding vibrations.
7) The laminations of both stator and rotor in SRM's experience magnetorestrictive forces. The forces can cause lamination vibration of the stator and rotor, with the problem being aggravated if the stator or rotor is not well stacked.
8) The torque ripple produced by many common control strategies is considerably larger in SRM's than those in many other motors. The torque ripple in fact is the tangential magnetic force exerted on the poles. It mainly excites stator vibrations.
9) The commutation of the tangential forces, which are exerted on the poles of the stator and rotor and produce torque, can excite the vibration of the stator and rotor.
10) There exists a strong concentrated radial magnetic attraction between stator and rotor poles, in particular in the SRM with doubly salient structures. This attractive force leads to stator vibrations.

Some of the above sources of acoustic noise in SRM's have been presented by many authors [1], [2] and examined in some depth by calculation or experiment [2]–[6]. It is widely accepted that the radial attractive force between stator and rotor is the dominant source of the vibration and acoustic noise in SRM's with doubly salient structures. However, the torque shifts among poles may not be omitted [7].

The existing research on acoustic noise can be mainly divided into two categories, frequency-domain methods [8]–[11] and time-domain methods [3], [6], [12]. The frequency-domain method is useful to show the spectrum and dominant components of the noise and vibrations. In addition, it can be used to predict the resonant frequencies in terms of the geometry of the motor. The time-domain method can reveal the links between acoustic noise, stator vibration, shape, and timing of the applied voltage and the current in the phase winding of the motor. To understand the effects of the power electronic converter on acoustic noise, the time domain is particularly useful.

In order to identify which factors affect the production of vibration and acoustic noise, experiments have been performed on existing SRM's of different designs [1]–[6]. The odd current harmonics, which coincide with the natural stator frequencies, excite the vibration modes more easily than even current harmonics coinciding with the natural resonant

Paper IPCSD 99–07, presented at the 1998 Industry Applications Society Annual Meeting, St. Louis, MO, October 12–16, and approved for publication in the IEEE Transactions on Industry Applications by the Electric Machines Committee of the IEEE Industry Applications Society. This work was supported by General Motors Corporate Research. Manuscript released for publication January 14, 1999.

The authors are with the Department of Electrical and Computer Engineering, Clarkson University, Potsdam, NY 13699 USA (e-mail: pillayp@clarkson.edu; wcai@clarkson.edu).

Publisher Item Identifier S 0093-9994(99)03840-2.

0093–9994/99$10.00 © 1999 IEEE

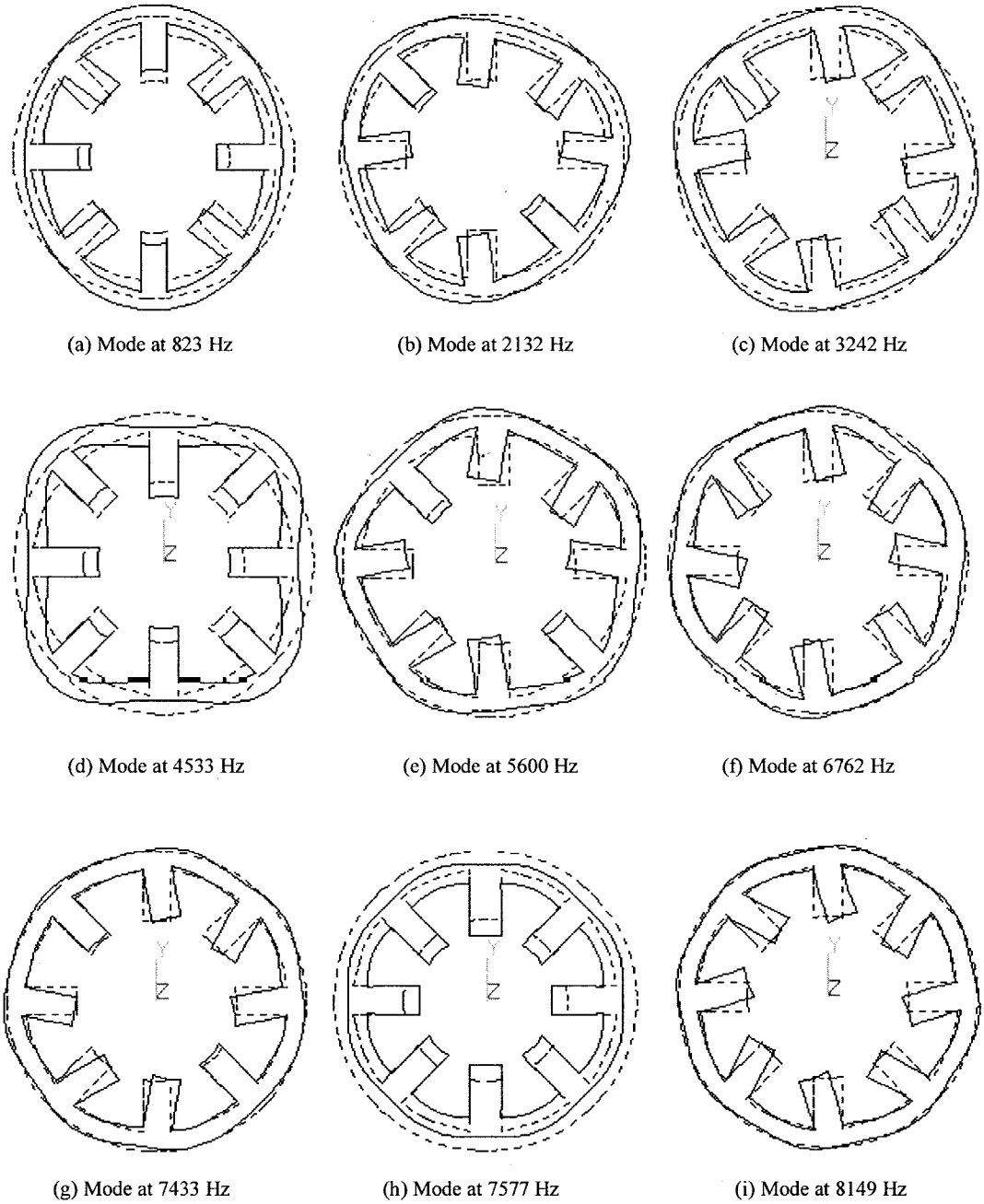

Fig. 1. Vibration modes of the stator laminations of SRM.

frequencies [2], [12]. The pure mechanical noise (bearing, windage and unbalance, etc.) in some motors is not significant. If the commutation of the phase current happens at or near the aligned position between stator and rotor axes, the acoustic noise is the most prominent. The torque ripple does excite some noise, but at a reduced level compared to the radial forces.

It has been shown that the structure and construction materials of the motor influence the nature of the stator vibration [3]. The magnitude of the radial force is a function of the phase current and rotor position. The current flowing through the phase windings depends on parameters such as phase number, lamination shape, resistance and inductance of the windings, etc., which are eventually fixed in the SRM and on variable parameters of the controller such as the supply voltage, turn-on and turn-off angles, current chopping condition, etc. The vibration induced behind a stator pole at 90° to the excited pole is exactly 180° out of phase with the vibration of the excited pole. The analysis and calculation of the magnetic forces and the dynamic response of the motor structure to these forces can be performed with the aid of a computer. This is examined in the following sections.

II. Vibration Analysis

Usually, the main stages of the analysis and calculation are as follows.

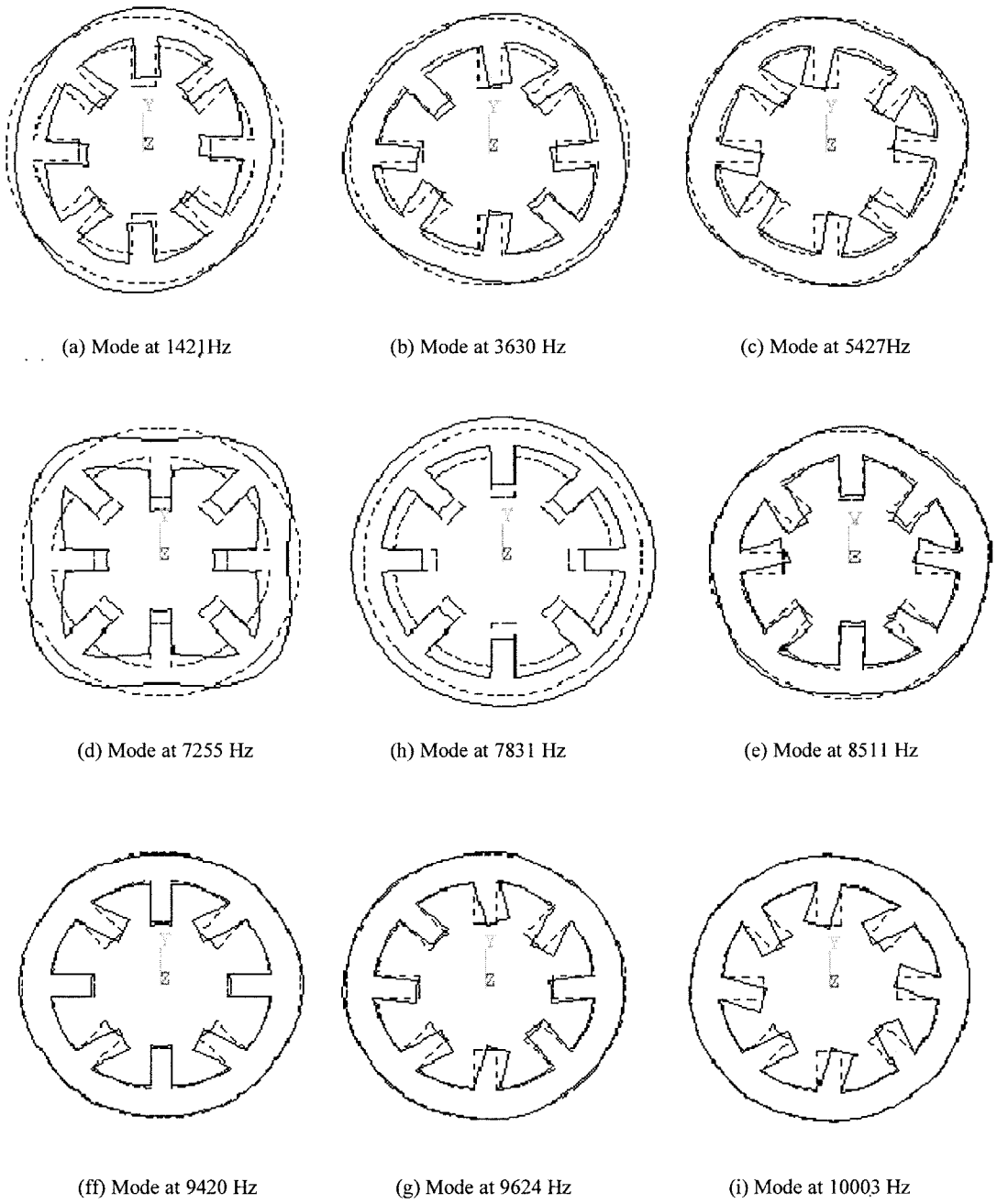

Fig. 2. Vibration modes of the stator laminations and smooth frame of SRM.

1) Component Natural Frequency Calculation and Verification: All of the mechanical components (stacked stator lamination, rotor, end shield, etc.) of the motor contribute to the acoustic noise and vibration and are required to be modeled. The natural frequency and mode shapes of the components such as stator and rotor can be assembled in the simulation software, either from a closed-form solution of analytical equations [8]–[11], [13] or from finite-element (FE) analysis. Because of the complexity of some components and nonlinear coupling between component structures, the calculated model needs to be verified empirically [5]. The COSMOS/M or ANSYS is capable of predicting the mode shapes and the corresponding natural frequencies of the three-dimensional (3-D) computer model of the components. The damping factor can be obtained with "impact tests" [5].

2) Calculation and Verification of the System Natural Frequency: After stage 1) is finished, the subassemblies (stator, rotor stack with shaft, etc.) model can be developed and the natural frequencies and mode shapes calculated. Finally, the entire model of the motor is assembled within the software package, the accuracy of which should be verified by test data.

3) Electromagnetic Model and Force Calculation: All the related dimensions, phase winding turns, and the properties of all materials are installed in a software package, for instance, ANSYS, ANSOFT, MAGNET, etc., to calculate the flux linkage curves as a function of rotor position and phase current. Usually, the two-dimensional (2-D) electromagnetic FE model

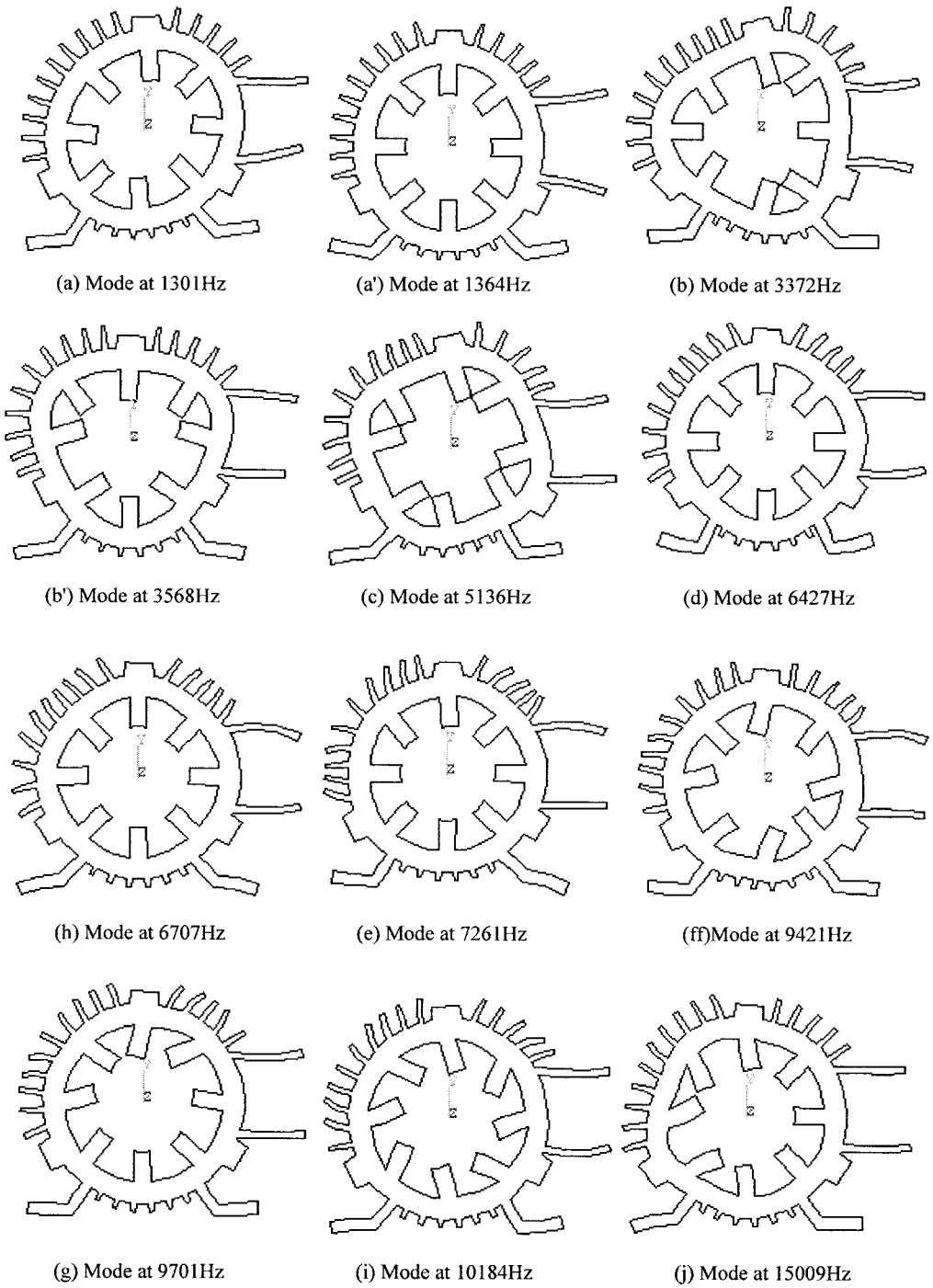

Fig. 3. Vibration modes of the stator laminations and frame with ribs.

is applied, perhaps with a correctional factor for the 3-D end effects [18]. According to the flux linkage curves and the other parameters of the SRM, as well as the operating parameters of the inverter controller, the current curves simulating the actual operation of the SRM can be obtained. Based on the current and rotor position, both radial and tangential forces are calculated. The vibration and acoustic noise are determined based on the results of the FE analysis. Of course, the time trace of the phase current from the measurement can also be applied as excitation in the FE model to calculate the electromagnetic forces of the motor.

4) System Dynamic Response Calculation and Verification: The calculated electromagnetic forces from the electromagnetic FE analysis are applied to the FE mechanical model so that the dynamic vibration response can be calculated. In this numerical analysis, the natural frequencies are obtained from the three FE calculations in step 1) and the damping coefficients of the components found by impact tests. It should be noted that the dynamic analysis could be performed on any individual component, but only the response of the complete motor model should be obtained for both the actual noise testing and accelerometer measurements on the motor.

TABLE I
MODAL FREQUENCY COMPARISON.

Mode	Laminations Stack			Smooth Frame		Ribbed Frame	
	FE (Hz)	AN (Hz)	%	(Hz)	%	(Hz)	%
a	823	788	- 4	1421	73	1301 1364*	58 66*
b	2132	2228	5	3630	70	3372* 3568	58* 67
c	3242	N/A		5427	74	5136	58
d	4533	4272	-6	7255	60	6427	42
e	5600	6908	23	8511	52	7261	30
f, ff	6762	N/A		9420		9421	
g	7433	N/A		9624	29	9701	31
h	7577	N/A		7831	3	6707	-11
i	8149	N/A		10003	23	10184	25

Note: AN is based on the analytical formula.

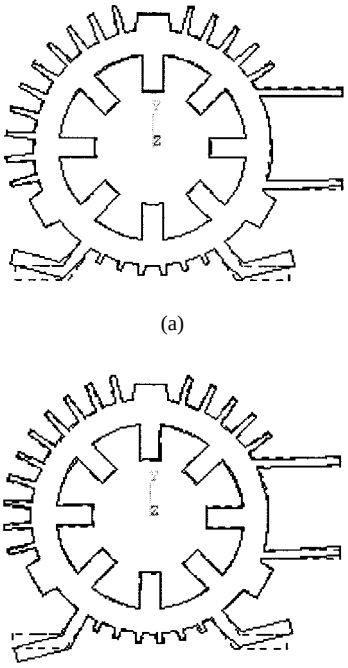

(a)

(b)

Fig. 4. Mode shapes between second and thirrd modes. (a) Mode shape at 1640 Hz. (b) Mode shape at 1756 Hz.

Steps 1) and 2) are addressed in this paper, which is the new contribution in this paper, with 3) and 4) left for future research.

III. VIBRATION MODES OF LAMINATIONS—SMOOTH FRAME AND RIBBED FRAME

The vibration modes and resonant frequencies calculated with the aid of an ANSYS FE package are given here for an 8-6 machine in Figs. 1(a)–(i). Some of the modes are easily exited by normal operation, while others would be difficult to excite. The resonant frequencies calculated from a structural FE analysis are listed in Table I. The normal forces excite the modes in Fig. 1(a), (d), and (e). The production of torque in the machine can excite the modes in Fig. 1(c) and (i). The other modes are excited by unsymmetrical excitation of the stator stack and are not considered here, although they may be excited during faulted conditions.

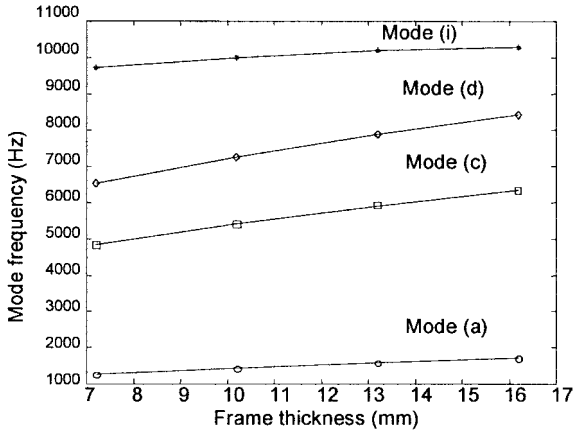

Fig. 5. Natural frequency versus frame thickness.

Although the radial electromagnetic forces are exerted on the stator teeth and poles, their vibration amplitude is much smaller than the amplitude of vibration of the stator yoke. An analytical method is presented here for the calculation of the resonant frequencies which concentrates on the natural vibration modes of the stator yoke. While the analytical formulas have been developed elsewhere, the new contribution here is the application to the SRM. The following assumptions are made in predicting the frequencies: 1) the stator yoke is a round rigid body; 2) the teeth and windings have no rigidity, so that their mass is attached to the yoke; 3) the periodic force waves with rth *order* are symmetrically exerted on the stator yoke ring; and 4) the only effects of all defects and notches is a reduction in the mass.

The following formula is used to predict the natural vibration frequencies for the force wave with rth order:

$$f_r = \frac{1}{2\pi}\sqrt{\frac{k_r}{m}} \tag{1}$$

where m is the equivalent mass per square meter (kg/m^2) on the cylindrical surface at the average yoke radius, which can be expressed by the following formula:

$$m = \frac{M_y}{2\pi R_{y(\mathrm{av})} L_{y(\mathrm{eff})}}. \tag{2}$$

Based on [15] and [16], the equivalent spring stiffness coefficient per square meter k_r (N/m^3) on the cylindrical surface at average yoke radius can be derived as

$$k_r = \begin{cases} \dfrac{Eh_y}{R^2_{y(\mathrm{av})}}, & \text{for } r = 0 \quad (3) \\ k_D, & \text{for } r = 1 \quad (4) \\ \dfrac{r^2(r^2-1)^2}{r^2+1}\dfrac{Eh_y^3}{12R^4_{y(\mathrm{av})}}, & \text{for } r \geq 2. \quad (5) \end{cases}$$

M_y is the yoke mass including stator windings and poles (kg), h_y is the yoke height in the radial direction (m), $R_y(\mathrm{av})$ is the average radius of yoke (m), $L_{y(\mathrm{eff})}$ is the effective length of yoke (m), k_D is the spring stiffness coefficient of the shock absorber under the motor ($k_D = 0$ without absorber),

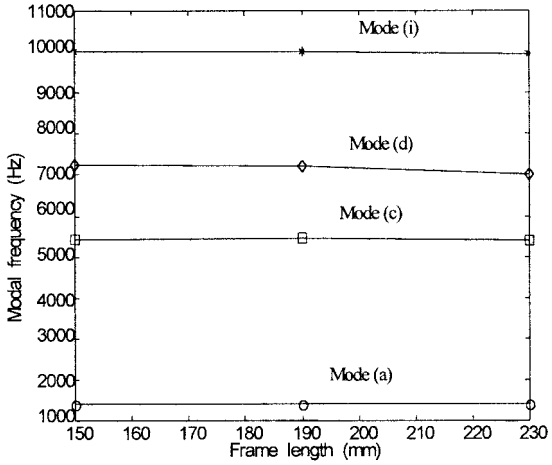

Fig. 6. Mode frequency versus frame length when lamination stack is fixed at 151 mm.

E is the elasticity modulus (N/m^2), and r is the order of electromagnetic force waves.

The dimensions of a 4-kW (5.5 hp) SRM are given as follows: $R_{\rm si} = 4.818 \times 10^{-2}$ m, $R_y = 7.84 \times 10^{-2}$ m, $R_{\rm so} = 8.98 \times 10^{-2}$ m, the pole arc of stator $\beta s = 20.2°$, pole number $N_s/N_r = 8/6$, length of stator laminations $L_y = 0.151$ m, the mass density of stator laminations $\rho_{\rm Fe} = 7800$ kg/m^3, Young's elasticity modulus $E = 2.07 \times 10^{11}$ N/m^2, winding area $A_w = 7 \times 24 \times 10^{-6}$ m^2, turns of windings $N = 56$ turns/pole, and specific mass of windings $\rho_c = 8.9 \times 10^3$ kg/m^3.

According to the above parameters, several natural vibration frequencies are obtained, as shown in Table I. Compared with the results using the FE method, the natural vibration frequencies using (1)–(5) have sufficient accuracy at the first four orders of the force waves, but several vibration modes and frequencies are missing between orders. In fact, these formulas are valid only under the limitation of $rh_y \ll R_{y(\rm av)}$.

For example, the analytical model is unable to predict mode c which the FE model predicts. This is because of the simplifying assumptions in the development of the analytical model.

This paper also considers the effects of the frame on the mode shapes and frequencies. A tight friction coupling between the laminations and frame is assumed, with the effects of the windings on the mode shapes and resonant frequencies neglected. While only the 2-D in-plane mode shapes are presented here, the calculations are based on a 3-D FE structural analysis.

Fig. 2 shows the effects of adding a smooth frame to the stator laminations. The thickness of the frame corresponds to that of a commercial machine for the modes given in Fig. 3(a)–(i). The first observation is that while several of the mode shapes that exist with the lamination only also exist with the lamination and frame, there is a reordering of the mode shapes in terms of frequency. While the first four mode shapes of the laminations are also the first four in the lamination and frame, for example, the mode shape at 7577 Hz [Fig. 1(h)] is shifted to the fifth mode shape in terms of frequency for the case of the lamination plus frame. The figures in Fig. 2 are presented in order of the increasing frequency, yet labeled

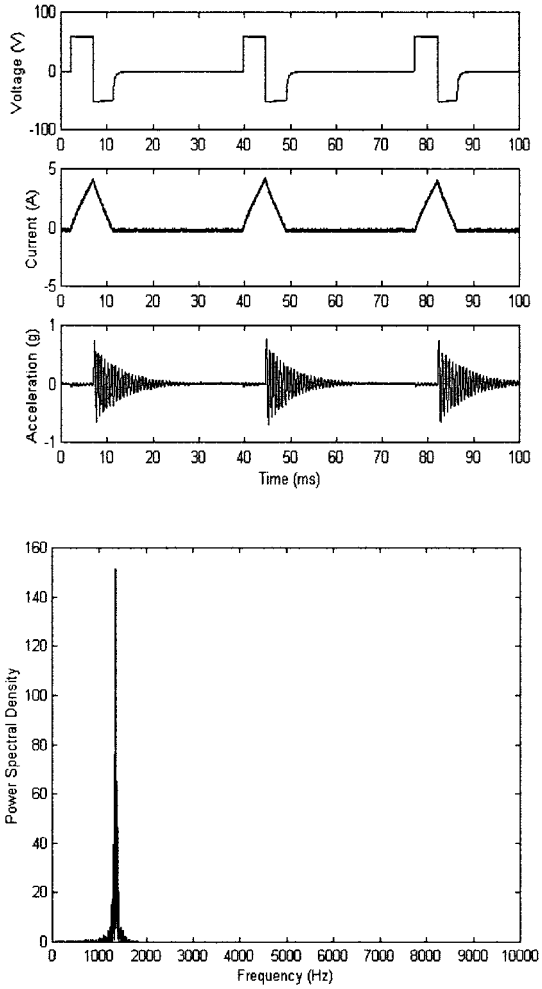

Fig. 7. Frequency spectrum under single-phase excitation (Repetition = 26.67 Hz) Vibration dominant frequency = 1340 Hz.

according to the base case in Fig. 1. Thus, Fig. 1(e), which is a mode at 5600 Hz, is shifted to 8511 Hz in Fig. 2 and is the sixth highest mode and not the fifth, as shown in Fig. 1(e). The mode in Fig. 1(f) has no correspondence in Fig. 2 and, similarly, for the mode in Fig. 2(ff). Where the mode shapes do coincide, there is a large increase in the frequency. For example, the mode in Figs. 2(a) and 1(a) occurs at 1421 Hz for the frame and lamination and at 823 Hz for the lamination alone, respectively, which is an increase of 73%. These frequencies of the smooth frame and laminations are presented in Table I along with the corresponding increase in frequency for that particular mode.

Commercial machines often use ribs for improved cooling. Fig. 3 shows the mode shapes and resonant frequencies when a ribbed frame is used. The particular mode shapes that are selected for Fig. 3 correspond to the same mode shapes of Fig. 2. The fins allow additional degrees of freedom in the motion of the frame/stack combination, thus creating the additional mode shapes. Two such cases are given in Fig. 4, which are mode shapes that occur between modes in Fig. 3(a) and (b). Some modes that are coincident in the lamination and lamination with smooth frame become separated in the ribbed design because the ribs are not symmetrical around the

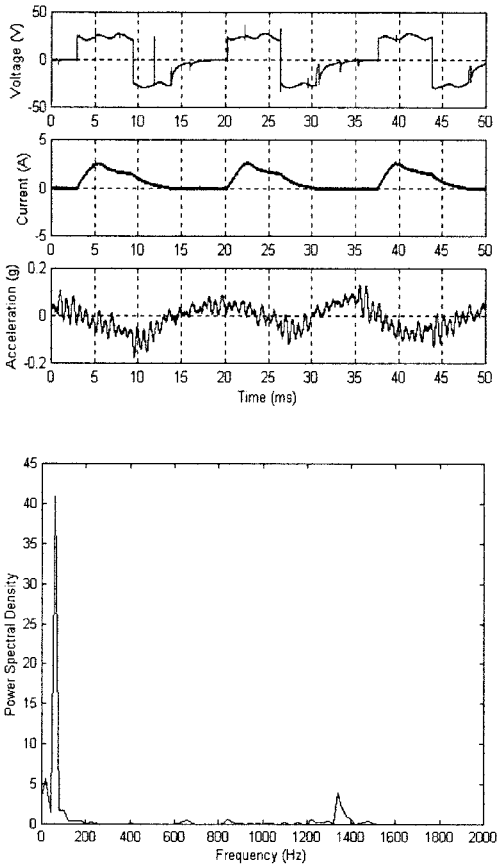

Fig. 8. Frequency spectrum under four-phase excitation (repetition $= 5 * 3.5$ ms). Dominant frequency $f = 57.5$ Hz, $f = 1360$ Hz.

periphery. For example, the first mode of the lamination and lamination plus frame are split into two separate modes for the case of the ribbed frame. This is given in Fig. 3(a) and (a′). Similarly, the mode of Fig. 2(b) is separated into the modes of Fig. 3(b) and (b′) for the case of a ribbed frame. These asymmetries are caused by the mounting feet, terminal block, and lifting hook, which are not modeled in the lamination stack or lamination stack with smooth frame. The corresponding frequencies and percentage changes with respect to the base case of a lamination only is give in Table I.

Given the influence of the frame on the natural frequency, it is, therefore, of interest to examine the effects of the frame thickness on the natural frequencies. Fig. 5 summarizes the results for the case of a z-constrained vibration of a smooth frame, showing a gradual increase in the frequencies of the mode shapes selected for analysis.

In practical machines, the frame length is often longer than the stack length to allow space for the end windings and, possibly, encoders. An analysis of the effects of increasing the frame length for a constant stack length of 151 mm is given in Fig. 6. Initially, there is a slight increase in the modal frequency up to 190 mm, but, subsequently, there is a decrease in the modal frequency.

A. Experimental Validation

The experimental validation of vibration results is a non-trivial task, requiring the use of accelerometers, screwed into the motor frame, preferably behind a pole for maximum sensitivity. This was done on a practical 5.5-hp commercial machine, with one phase pulsed by a square-wave voltage given in Fig. 7 to allow excitation of the second mode shape. The period of the excitation is chosen to be much larger than the time required for the output of the accelerometer to decay nearly to zero. The amplitude of the exciting voltage is chosen to allow the resulting current to produce a large enough force for vibration measurement. The resulting triangular current and accelerometer output are given, as well as the power spectral density of the accelerometer output shown in Fig. 7.

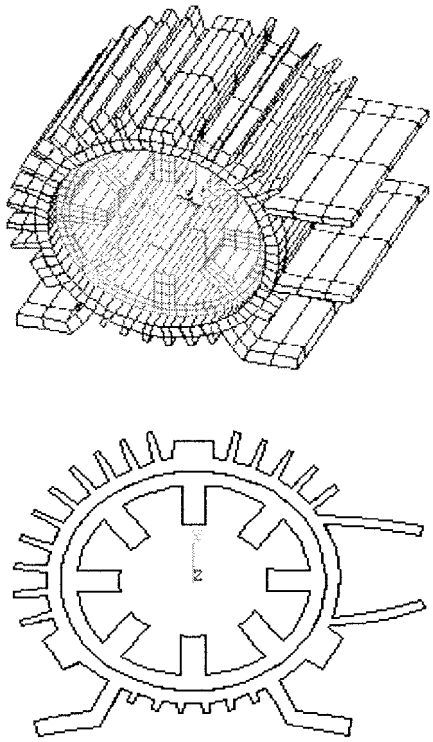

Fig. 9. Predicted mode shape at 1364 Hz.

The frequency of resonance that is excited is 1340 Hz, which corresponds closely to the predicted modal frequency of 1364 Hz given in Fig. 9. Similarly, the motor running at a low speed of 575 r/min also excites this mechanical mode, as shown in Fig. 8. This speed is sufficiently lower than the frequency of the second-order mode shape which would excite the second mode shape vibration. In addition, a vibration corresponding to the fundamental excitation frequency is also evident in Fig. 8.

IV. Conclusion

This paper has conducted an in-depth study of the vibration modes of the stator of switched reluctance machines with both the FE analysis and an analytical method. The study started with the laminations and was then extended to a smooth frame, as well as a ribbed frame. The first few modes of the laminations were also predicted using an analytical formula with the disadvantage that simplifying assumptions necessary to make the problem tractable can lead to an inability in predicting certain modes. While the first few mode shapes remain the same, as one goes from the lamination to the

smooth frame, there is a large increase in the corresponding frequency. There is also a change in the order of the mode shapes. The resonant frequencies of the low-order modes decrease due to the existence of the frame ribs and keys. This means that the ribs and keys mainly add extra mass to the stator vibration system for the low-order modes, so that their effects can be considered as extra mass. However, an increase occurs in the higher order resonant frequencies. This means that the effects of ribs and keys mainly contribute extra stiffness to the high-order mode shapes of the stator vibration system. This conclusion contradicts the results of previous papers and explains why it is not permissible to simply consider the ribs, etc., as an extra mass. The addition of ribs, feet, and the termination block to the frame introduces numerous additional vibrating modes. Modes that are coincident in the symmetrical cases of the lamination or lamination with smooth frame become separated in the unsymmetrical machine.

The effects of changing the thickness and length of the frame were also examined, with length having less of an effect than thickness.

The results on a practical 5.5-hp SRM of ribbed frame design confirm some of the predictions with reasonable accuracy.

ACKNOWLEDGMENT

The authors acknowledge N. Boules for technical support, Y. Liu for help with the measurements, G. Ahmadi for help with the analytical work, and R. D. Pillay for helping with the preparation of the paper.

REFERENCES

[1] R. S. Colby, F. Mottier, and T. J. E. Miller, "Vibration modes and acoustic noise in a 4-phase switched reluctance motor," in *Conf. Rec. IEEE-IAS Annu. Meeting*, Lake Buena Vista, FL, Oct. 8–12, 1995, vol. 1, pp. 441–447.

[2] D. E. Cameron, J. H. Lang, and S. D. Umans, "The origin and reduction of acoustic noise in doubly salient variable-reluctance motors," *IEEE Trans. Ind. Applicat.*, vol. 28, pp. 1250–1255, Nov./Dec. 1992.

[3] Y. Tang, "Characterization, numerical analysis and design switched reluctance motor for improved material productivity and reduced noise," in *Conf. Rec. IEEE-IAS Annu. Meeting*, San Diego, CA, Oct. 6–10, 1996, vol. 1, pp. 715–722.

[4] A. Michaelides and C. Pollock, "Reduction of noise and vibration in switched reluctance motors: New aspects," in *Conf. Rec. IEEE-IAS Annu. Meeting*, San Diego, CA, Oct. 6–10, 1996, vol. 1, pp. 771–778.

[5] J. Mahn, D. Williams, P. Wung, G. Horst, J. Lloyd, and S. Randall, "A systematic approach toward studying noise and vibration in switched reluctance machines: Preliminary results," in *Conf. Rec. IEEE-IAS Annu. Meeting*, San Diego, CA, Oct. 6–10, 1996, Vol. 1, pp. 779–.

[6] C. Y. Wu and C. Pollock, "Time domain analysis of vibration and acoustic noise in the switched reluctance drive," in *Proc. Inst. Elect. Eng. 6th Int. Conf. Electrical Machines and Drives*, London, U.K., 1993, pp. 558–563.

[7] W. Cai and J. Li, "Several methods and design considerations to reduce the vibration and noise of switched reluctance motors," Harbin Inst. Elect. Technol., Harbin China, Res. Rep., Dec. 1990, pp. 166–178.

[8] R. S. Girgis and S. P. Verma, "Experimental verification of resonant frequencies and vibration behavior of stators of electrical machines, part I-models, experimental procedure an apparatus," *Proc. Inst. Elect. Eng.*, vol. 128, pt. B, no. 1, pp. 12–21, Jan. 1981.

[9] S. P. Verma and R. S. Girgis, "Experimental verification of resonant frequencies and vibration behavior of stators of electrical machines, part II-experimental investigations and results," *Proc. Inst. Elect. Eng.*, vol. 128, pt. B, no. 1, pp. 22–32, Jan. 1981.

[10] S. P. Verma and R. S. Girgis, "Resonance frequencies of electrical machines stator having encased construction, part I: Derivation of the general frequency equation," *IEEE Trans. Power App. Syst.*, vol. PAS-92, pp. 1577–1585, Sept./Oct. 1973.

[11] S. P. Verma and R. S. Girgis, "Resonance frequencies of electrical machines stator having encased construction, part II: Numerical results and experimental verification," *IEEE Trans. Power App. Syst.*, vol. PAS-92, pp. 1586–1593, Sept./Oct. 1973.

[12] C. Y. Wu and C. Pollock, "Analysis and reduction of acoustic noise and vibration in the switched reluctance drive," *IEEE Trans. Ind. Applicat.*, vol. 31, pp. 91–98, Jan./Feb. 1995.

[13] S. P. Verma and R. S. Girgis, "Method for accurate determination resonant frequencies and vibration behavior of stators of electrical machines," *Proc. Inst. Elect. Eng.*, vol. 128, pt. B, no. 1, pp. 1–11, Jan. 1981.

[14] P. Pillay, R. M. Samudio, M. Ahmed, and P. T. Patel, "A Chopper-controlled SRM drive for reduced acoustic noise and improved ride-through capability using supercapacitor," *IEEE Trans. Ind. Applicat.*, vol. 31, pp. 1029–1038, Sept./Oct. 1995.

[15] S. Chen, *Electrical Machinery Design*, 1st ed. Beijing, China: Machinery Industry Press, 1982.

[16] R. D. Blevins, *Formulas for Natural Frequency and Mode Shape*. New York: Van Nostrand Reinhold, 1979, p. 205.

[17] W. C. Young, *Roark's Formulas for Stress & Strain*, 6th ed. New York: McGraw-Hill, 1989.

[18] A. V. Radun, "Design considerations for the switched reluctance motor," *IEEE Trans. Ind. Applicat.*, vol. 31, pp. 1079–1087, Sept./Oct. 1995.

Pragasen Pillay (S'84–M'87–SM'92) received the Bachelor's degree from the University of Durban-Westville, Durban, South Africa, in 1981, the Master's degree from the University of Natal, Durban, South Africa, in 1983, and the Ph.D. from Virginia Polytechnic Institute and State University, Blacksburg, in 1987, while funded by a Fulbright Scholarship.

From January 1988 to August 1990, he was with the University of Newcastle upon Tyne, Newcastle upon Tyne, U.K. From August 1990 to August 1995, he was with the University of New Orleans, New Orleans, LA. He is currently a Professor in the Department of Electrical and Computer Engineering, Clarkson University, Potsdam, NY, where he holds the Jean Newell Distinguished Professorship in Engineering. His research and teaching interests are in modeling, design, and control of electric motors and drives.

Dr. Pillay is a member of the IEEE Power Engineering, IEEE Industry Applications, IEEE Industrial Electronics, and IEEE Power Electronics Societies. He is a member of the Electric Machines Committee, Vice Chairman-TRANSACTIONS Paper Reviews of the Industrial Drives Committee, and Vice Chairman of the Continuing Education Committee within the IEEE Industry Applications Society. He has organized and taught short courses in electric drives at the Annual Meeting of the Industry Applications Society. He is a member of the Institution of Electrical Engineers, U.K., and a Chartered Electrical Engineer in the U.K.

William (Wei) Cai was born in Shantung, China. He received the B.Sc. and M.Sc. degrees in electrical engineering from Harbin University of Science and Technology [HUST, formerly Harbin Institute of Electrical Technology (HIET)], Harbin, China, in 1982 and 1985, respectively. He is currently working towards the Ph.D. degree in electrical engineering at Clarkson University, Potsdam, NY.

In 1985, he joined the Department of Electrical Engineering, HIET, as an Instructor Associate. He was promoted to Lecturer and Associate Professor at HIET in 1987 and 1990, respectively. He was an Honorary Research Fellow at WEMPEC, University of Wisconsin, Madison, in 1995. He was an Electrical Engineer at the Institute of Electrical Machines, ETH-Zurich, Zurich, Switzerland, in 1996. He is engaged in research and development of electrical machine and power electronics products. His interests include design, control, and modeling of electrical machines and drives, numerical computation of magnetic fields and mechanical structures, vibration and noise analysis of electrical motors, and digital signal processing.